Aalborg Universitet

AALBORG UNIVERSITY
DENMARK

Geometrical Optimization for Improved Power Capture of Multi-Level Overtopping Based Wave Energy Converters

Margheritini, Lucia; Victor, L.; Kofoed, Jens Peter; Troch, P.

Published in:
Proceedings of the International Offshore and Polar Engineering Conference

Publication date:
2009

Document Version
Publisher's PDF, also known as Version of record

Link to publication from Aalborg University

Citation for published version (APA):
Margheritini, L., Victor, L., Kofoed, J. P., & Troch, P. (2009). Geometrical Optimization for Improved Power Capture of Multi-Level Overtopping Based Wave Energy Converters. *Proceedings of the International Offshore and Polar Engineering Conference*, 339-344.
http://www.isope.org/publications/proceedings/ISOPE/ISOPE%202009/data/papers/2009-TPC-397.pdf

General rights
Copyright and moral rights for the publications made accessible in the public portal are retained by the authors and/or other copyright owners and it is a condition of accessing publications that users recognise and abide by the legal requirements associated with these rights.

- Users may download and print one copy of any publication from the public portal for the purpose of private study or research.
- You may not further distribute the material or use it for any profit-making activity or commercial gain
- You may freely distribute the URL identifying the publication in the public portal -

Take down policy
If you believe that this document breaches copyright please contact us at vbn@aub.aau.dk providing details, and we will remove access to the work immediately and investigate your claim.

Geometrical Optimization for Improved Power Capture of Multi-level Overtopping Based Wave Energy Converters

L. Margheritini[1], L. Victor[2], J. P. Kofoed[1], P. Troch[2]
[1]Department of Civil Engineering, Aalborg University, 9000 Aalborg, Denmark
[2]Department of Civil Engineering, Ghent University, 9000 Ghent, Belgium

ABSTRACT

In multi-level wave energy converters the water from incoming waves is stored in reservoirs one on top of the other. Prevision formula for the overtopping flow rates in the individual reservoirs is fundamental for dimensioning correctly the turbines and optimizing the device. Having a number of reservoirs one on top of each other means that the representative overtopping formulae for coastal structures are not sufficient to describe the phenomena. This paper proposes to describe the dependence of the overtopping on a new parameter which is the horizontal distance between the reservoirs or, in other words, the opening between two consecutive reservoirs. 13 different geometries have been tested in 2D irregular waves and a new formulation for prediction of overtopping in multilevel structures is presented.

KEY WORDS: Overtopping; wave energy converters, 2D testing, irregular waves, crest levels; optimization; power capture.

INTRODUCTION

Wave energy converters (WECs) based on the overtopping principle utilize the potential energy of incoming waves by storing the overtopping water in reservoirs where specifically design low head hydro turbines convert the available potential power. Some advantages have been foreseen for such a kind of devices over different WE technologies: in first place the derived electricity is characterized by small fluctuations because the conversion from wave energy to potential energy can benefit of a relatively calm water in the reservoirs. In second place the economics as well as the environmental impact of the device can be shared with other coastal facilities such as breakwaters. Despite the application on breakwater not being a prerogative of overtopping wave energy converters, these devices are the only ones that can contribute to improve the water quality in closed harbours with the seawater ejected from the turbine outlet. WECs based on the overtopping principle are Wave Dragon (Kofoed 2006a), Wave Plane (Frigaard 2008) and SSG (Margheritini 2008a). Considerable increase in stored energy from the overtopping water can be obtained by using multilevel devices (Kofoed 2006b); moreover this is the most effective solution for fix overtopping devices that can not adapt the crest free boards to the sea state by changing the buoyancy level like in Wave Dragon device. In the design of an overtopping device the main parameter to be defined are the crest free boards R_{cj}, j=1,2...n, n=number of reservoirs. These levels are defined through an iteration process that leads to maximization of hydraulic efficiency defined as:

$$\eta_{hyd} = \frac{\sum_{j=1}^{n} \rho g q_j R_{cj}}{\frac{\rho g^2}{64\pi} H_s^2 T_E} = \frac{P_{crest}}{P_{wave}} \quad (1)$$

Where ρ=1020 kg/m^3, g = 9.82 m/s^2, H_S is the significant wave height and T_E is the energy period = $m\text{-}1/m_0$, where m_n is the n-th moment of the wave spectrum. $R_{c,j}$ is the crest level of the respective reservoir and $q_{ov,j}$ is the total overtopping flow rate for the j-reservoir.
The parameters influencing the overtopping are well known and they include both effects of the wave climate as well as of the structure geometry (Van der Meer and Janssen 1995; Franco et al. 1995). A specific study on the influence of oblique waves and directional spreading has been done for fix geometry of specific multi-level WEC with good accordance of results with literature (Margheritini 2008b). The expression available now to calculate q_j in Eq. 1 is the integration of the derivative overtopping discharge with respect to the vertical distance z (Kofoed 2002):

$$\frac{dq/dz}{\sqrt{gH_S}} = Ae^{B\frac{z}{H_S}} e^{C\frac{R_{c,1}}{H_S}} \quad (2)$$

The coefficients A, B and C are fitted from laboratory tests, q is the average overtopping discharge per width [m^3/s/m], z is the vertical distance from the s.w.l., g is the gravity acceleration, H_s is the significant wave height, and R_{c1} the crest free board of the lower reservoir.
Nevertheless the structure geometry of multi-level WECs is such to require the introduction of new parameter to describe the overtopping into the reservoirs. From a comparison of the calculated and measured q_j during 2D physical model tests it emerged that Eq. 2 is imperfect in the description of the phenomena when varying the horizontal distance HD from the ranges in which Eq. 2 has been established. In other words it seams necessary to introduce a new relation expressed by:

$$\frac{dq/dz}{\sqrt{gH_S}} = f_1\left(\frac{z}{H_S}, \frac{R_{c,1}}{H_S}, HD^*\right) \quad (3)$$

In Eq. 3 *HD** is the adimensionalized horizontal distance between the opening of two consecutive levels (Fig 1).
The purpose of this paper is to define the effect of the horizontal distance *HD* on the overtopping discharge and find a parameter to be added in the existing formula that can include this effect.

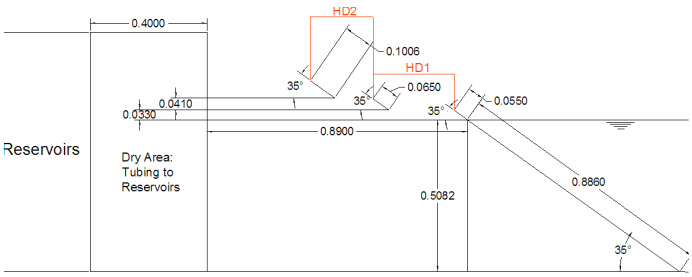


Figure 1. Definition sketch. measures in meters, side view.

TESTS SET UP

Tests in scale 1:30 of the North Sea conditions have been carried out in the shallow water wave flume at the Hydraulics and Coastal Engineering laboratory of the Department of Civil Engineering of Aalborg University. The flume is 25 m long, 1.5 m wide and 1 m deep. The flume is equipped with a piston type wave generator with a stroke length of approximately 70 cm. The wave generator is controlled by a PC-controlled DHU Servo Amplifier. The standard generation software is AWASYS, which is an active absorption system that can be used to generate both regular and irregular waves. AWASYS is developed in the laboratory.
The model was placed at the end of the flume, in center position occupying 0.514 m of in width (Fig. 2). Approximately 2 m long leading walls to the model assured pure 2D waves. At the sides of the model outside the leading walls an artificial dissipating beach was realized.
The multi-level model structure consisting of 3 horizontal metal plates with fronts inclined of 35° as it has been demonstrated that this is the optimal value for maximization of overtopping (Le Mèhautè et al. 1968, and Kofoed 2002). The plates can be dismounted to vary the number of reservoirs from 1 to 3 and can slide one respect to the others in order to change the horizontal distances *HD1* and *HD2* (Definition sketch, Fig. 1). The majority of the tests have been carried out with 2 levels and results will be presented only for this configuration. 13 different geometries with 0.30 m. <HD1<0.053 m. have been testes.
The crest levels R_{c1} and R_{c2} are fixed respectively at 0.0333 m., 0.0716 m. from mean water level (m.w.l.). A wooden run-up ramp 0.886 m. long inclined of 35° leads the waves to the model.

Wave conditions

2D irregular waves from the Jonswap spectrum (3.3 peak enhancement constant) have been generated during the tests with water depth = 0.51 m. in front of the structure. Tested wave conditions are presented in Table 1. Each tests lasted 30 minutes. Wave conditions have been selected among the most common in the North Sea (probability of occurrence > 5%), (W1, 2, 3, 4 in Table 1). Additionally, different conditions have been investigated by changing T_p for the same H_S (W1a, W2a,b; W3b,c; W4b,c in Table 1) in order to investigate the effect of the wave steepness:

$$s_0 = \frac{2\pi H_S}{gT_P^2} \qquad (4)$$

Table 1. Tested conditions, model scale.

Name	Hs [m]	Tp [s]	s0
W1	0.033	1.022	0.020403
W1a	0.033	2.066	0.004997
W2	0.067	1.278	0.026116
W2a	0.067	2.922	0.004996
W2b	0.067	0.924	0.049961
W3	0.100	1.534	0.027204
W3b	0.100	1.132	0.049932
W3c	0.100	2.531	0.009988
W4	0.133	1.789	0.026649
W4b	0.133	1.307	0.049941
W4c	0.133	2.922	0.009992

Wave measurements

Generated waves have been measured with 3 wave gauges in front of the structure, the closest one distanced 1.96 m. from the model, allowing the separation of incident and reflected waves according to the Mansard & Funke´s method (1980). The data acquisition was at 50 Hz. For the wave analysis the software WaveLab 3 has been used developed at Aalborg University.

Overtopping measurements

The water overtopping the crest levels was temporary stored in rear tanks after passing the tubing section (refer to Fig. 2). To each level corresponds one rear tank equipped with pumps of known performance and wave gauges for measuring the water level inside the tanks. The pumps were automatically emptying the tanks by pumping back in the basin when the water reached a pre-established level. By the total utilization of the pumps and the records of water levels inside the rear tanks, the overtopping volumes and flow rates q_j have been derived for the single reservoirs during each test. Final data were the average overtopping discharges over the generated sea state for each test.

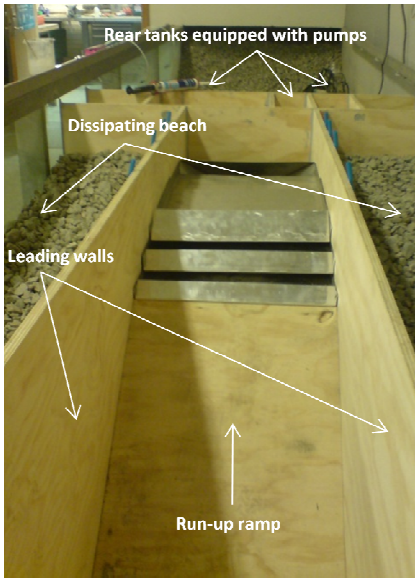


Figure 2. Front view of the model with 3 levels mounted.

RESULTS

When waves overtop the structure they showed surging behavior. The water first runs up the slope leading to the structure then the front of the first reservoir and if the wave is big enough, also the second front resulting in a cascade into the reservoir (Fig 3).
Following results are presented in terms of average overtopping discharge for each level with comparison with existing formulae.

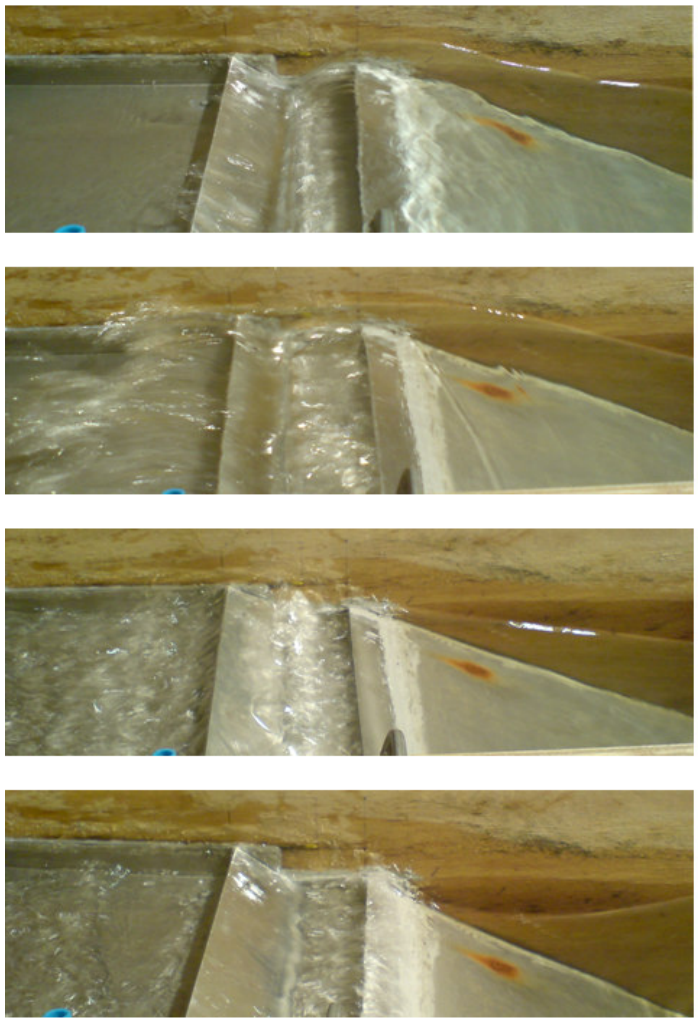


Figure 1. Overtopping event for wave condition W3, 2 levels model with HD1=0.11 m.

Influence of wave climate

The overtopping in the first reservoir appears to be slightly dependent on the wave steepness S_0 when plotting the results excluding wave condition W1 (Fig. 4). This wave condition has been excluded from Fig. 4 because responsible of very low overtopping rates and therefore misleading the overall results. It seams as if there is a parabolic trend for all the different geometries, with lower overtopping for smaller *HDs*. Trend lines have been added for HD1=0.07, 0.10, 0.15 and 0.20 m. in Fig. 4. The higher overtopping occurs for values of $S_0 \approx 0.022$.

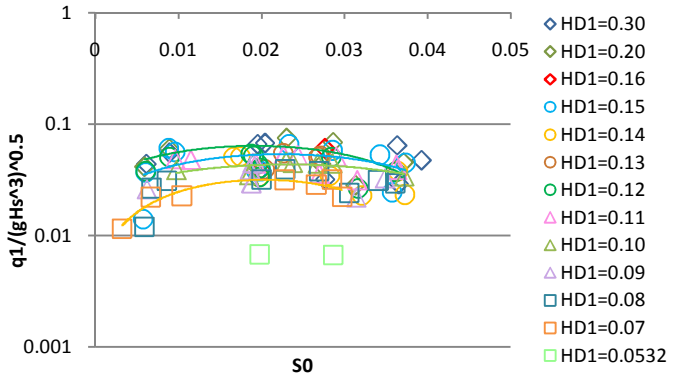


Figure 2. Adimensionalized overtopping in the lower reservoir for different geometries, plotted against the wave steepness S_0, logarithmic scale. *HD1* in meters.

Distinct behavior can be recongnized for all the tested geometries when plotting the adimensionalized discharge against the adimensionalized *HD1* (Fig. 5). Trend lines have been added for HD1=0.07, 0.11, 0.15 and 0.30 m. in Fig. 5. This emphasizes that there is an effect of the parameter *HD1* on the overtopping on the first reservoir, with a linear trend for all the geometries. Obviously it is common for all *HDs* that the higher overtopping occurs for higher waves (small HD/H_S).
For the same values of *HD1* the higher overtopping will occur for the geometry that features the less obstruction to the reservoir, i.e. for the larger *HD1*. For the specific data set, the higher overtopping in the first reservoir occurs for $HD/H_S \approx 3$ corresponding to *HD1*>0.15 m.. Those represent the conditions when the top level is not interfering with the water capture in the level below. For $HD/H_S<2$ the upper level has an influence on the water storage capturing indeed part of the water that would have instead been stored in the lower reservoir.

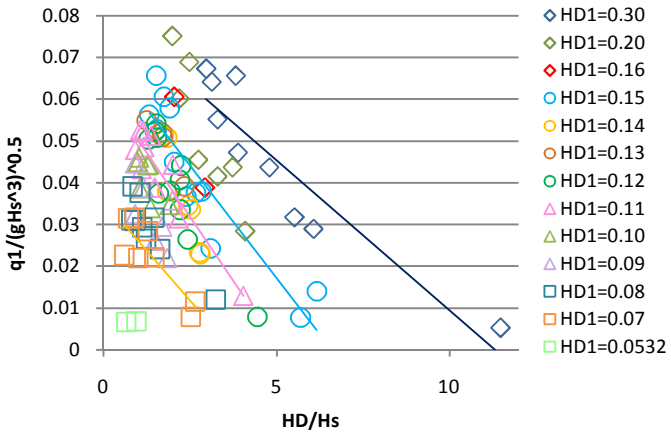


Figure 3. Adimensionalized overtopping in the lower reservoir for different values of *HD*, plotted against the adimensionalized *HD*. *HD1* in meters.

For the higher reservoir all the geometries follow the same trend (Fig. 6) with opposite behavior from the lower reservoir: higher overtopping occurs for *HD*< 0.12m. but the overtopping goes quickly to 0 for $HD/H_S>2$. Those are the cases where the upper level is caching part of the overtopping that would instead end entirely in the lower reservoir id *HD1* was bigger. It is anyway difficult to delineate a threshold with regard to the geometry that indicates when the upper level starts having

an effect on the water capture and not much difference can be appreciated for *HD1*=0.13 and 0.14 m.
These differences on the overtopping trends for the two reservoirs must be explained considering that the overtopping in the lower reservoir is not completely open but partially close by the above level.

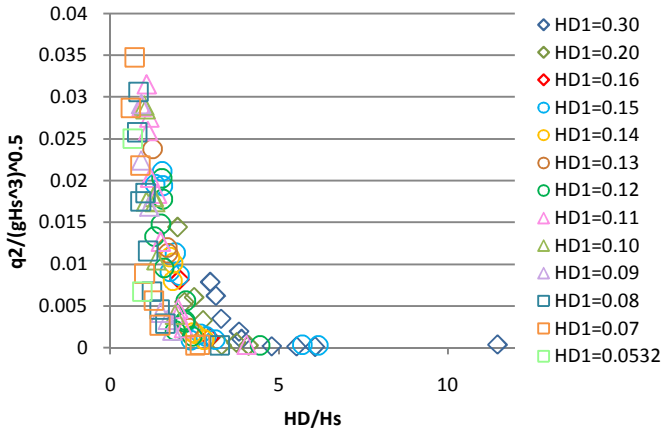


Figure 4. Adimensionalized overtopping in the upper reservoir for different values of *HD*, plotted against the adimensionalized *HD*. *HD1* in meters.

Comparison with prediction formulae

At first the overtopping of the two reservoirs have been summed up and related to the crest freeboard of the lowest reservoir. Results are shown as a comparison between measured and calculated data from Kofoed 2002, Eq. 2 , with *A*=0.197, *B*=-1.753 and *C*=-0.408 (Fig 7).

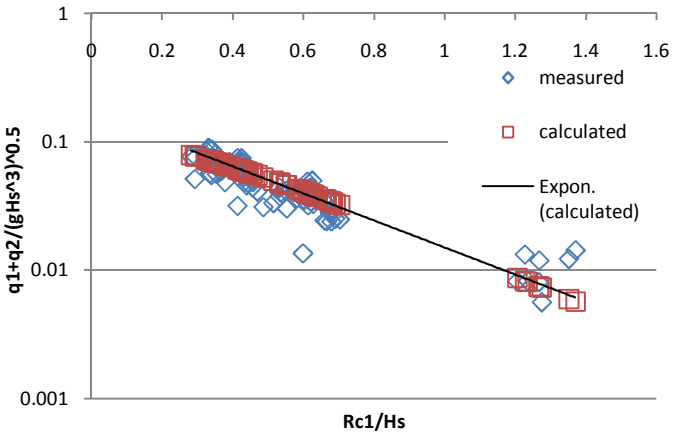


Figure 5. Adimensionalized total overtopping discharge as a function of dimensionless freeboard: comparison between measured and calculated data.

In general a good accordance can be noticed apart for few points: the prediction formulae overestimate the overtopping for those tests with the smallest *HD* while it underestimate the overtopping for some tests with high R_{c1}/H_s value. From a closer look the reasons behind the overestimation are clear as when *HD1* is very small it means the structure behaves like a single level but with a crest freeboard equal to $R_{c,2}$. The underestimated points instead correspond to wave condition W1a, where the period is particularly high despite waves being small. It is indeed possible to notice that when plotting the adimensionalized overtopping discharges from tests of different representative wave condition (Fig. 8), the overtopping measured in the lower reservoir increases depending on the *HD* while the overtopping in the upper reservoir decreases.
Both the overtopping rates have an upper limit that is given by the equation from Van der Meer and Janssen (1995) with coefficient λ_s added by Kofoed 2002 to take care of small Rc/Hs values, calculated for R_{c1} and R_{c2}:

$$\frac{q}{\lambda_S\sqrt{gH_S^3}} = 0.2e^{-2.6\frac{R_c}{H_S}\frac{1}{\gamma_r\gamma_b\gamma_h\gamma_\beta}} \quad (5)$$

Where the γ coefficients have been introduced to take into account the influence of geometric parameters and angle of wave attack.

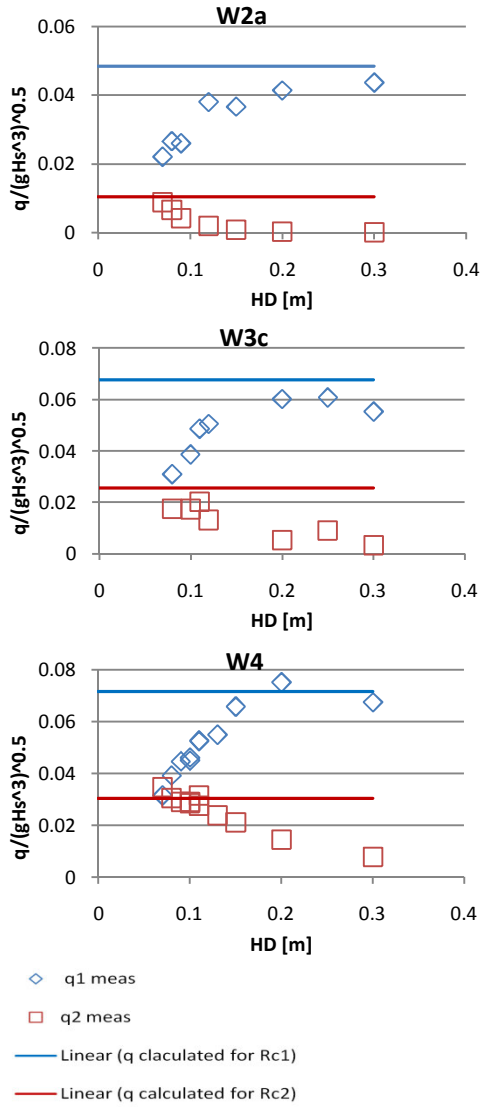


Figure 6. Overtopping discharges measured in low (q1) and top (q2) reservoirs for selected representative wave conditions, for different *HDs* with upper limits calculated for R_{c1} (upper line) and R_{c2} (lower line) from Eq.6.

ANALYSIS OF RESULTS

The results from each reservoir are presented separately and compared to prediction formulae derived from Eq. 2. Discordance have been underlined and it appeared clear that by taking into consideration the new parameter *HD* two different formulations of the overtopping prediction formula are needed, one for each reservoir, as the phenomena behind overtopping events in the first and second reservoir is different due to the presence or not of a roof i.e. the above reservoir. For this reason 2 coefficients to be implemented in Eq. 2 have been derived, one for each reservoir.

For the lower reservoir the prediction formula overestimates the overtopping for the tests with smallest *HD1* (Fig. 9). For the majority of the other data points the prediction formula underestimate the overtopping into the reservoir the more as the distance *HD1* increases. The only points that are correctly predicted are the ones with *HD1*=0.07 m which is indeed the value for which the formulation has been established.

For the second reservoir we don´t have good accordance and measured values are drawn from the prediction formula for all the cases (Fig. 10). In particular we have overestimation of the formula for all the *HD*>0.15 m. and underestimation for *HD*<0.11 m.

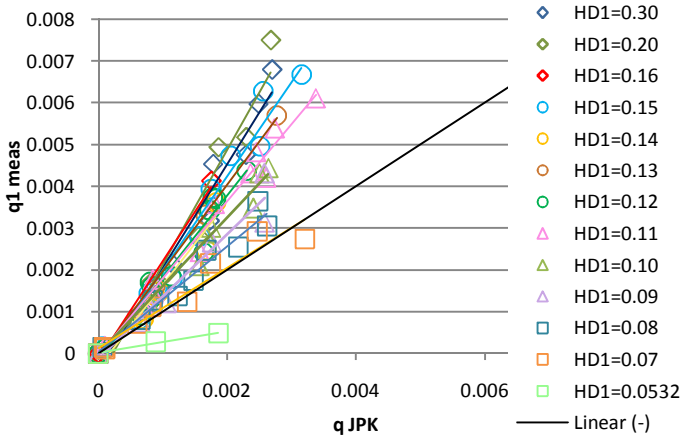


Figure 7. Comparison of measured and calculated values for different *HD1* for the lowest reservoir. *HD1* in meters.

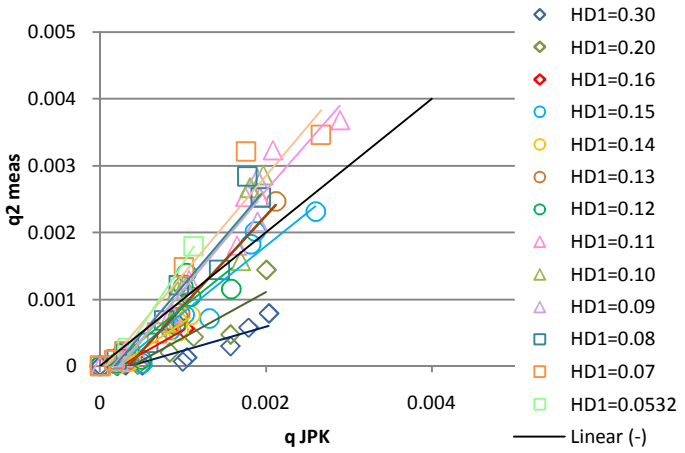


Figure 8. Comparison of measured and calculated values for different *HD1* for the higher reservoir. *HD1* in meters.

Linear curves with angular coefficients varying depending on *HD* show good agreement with the trend of the data with values of R-squared between 0.94 and 1 for the lower reservoir and between 0.81 and 1 for the second reservoir; in this last case the bigger discrepancies are for higher values of *HD* while for *HD*<0.15 m the agreement is satisfactory. A coefficient to be added at Eq. 2 has been defined and its equation found by mean of regression analysis (Fig. 11) in the form of second order logarithm that gives a value of R-squared = 0.99:

$$\lambda 1_{HD} = a + b\ln\left(\frac{HD}{R_{C1}}\right) + c\ln\left(\frac{HD}{R_{C1}}\right)^2 \qquad (6)$$

Where a=-1.15191, b=3.39915 and c = -0.76366.

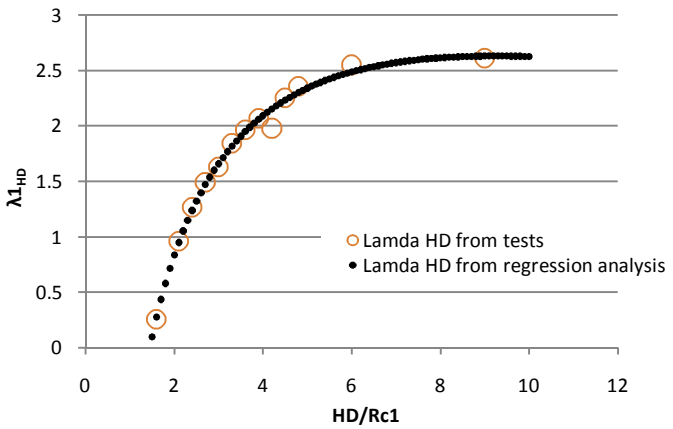


Figure 9. Dependency of the new coefficient $\lambda 1_{HD}$ on the HD/R_{c1}. The black curve have been calculated after Eq. 6. While the empty marks are derived from the tests.

For the second reservoir in the same way we have:

$$\lambda 2_{HD} = a\left(\frac{HD}{R_{C1}}\right)^2 + b\left(\frac{HD}{R_{C1}}\right) + c \qquad (7)$$

Where a=0.024061, b=-0.45563 and c = 2.50675 that gives a agreement expressed by R-squared =0.89.

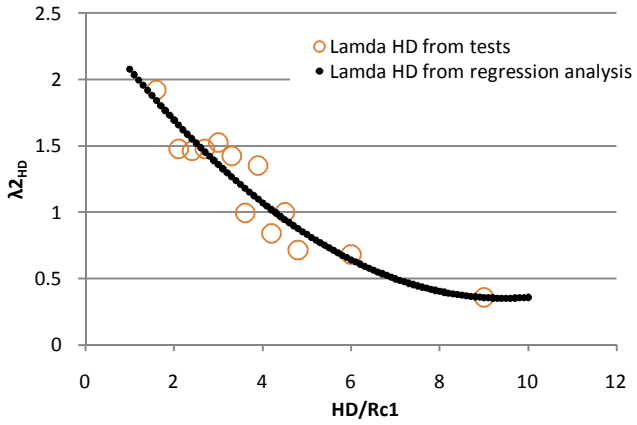


Figure 12. Dependency of the new coefficient $\lambda 2_{HD}$ on the HD/R_{c1}. The black curve have been calculated after Eq. 7. While the empty marks are derived from the tests.

We have now two different formulae for the overtopping in the first and in the second reservoir; rewriting Eq. 2 results in:

$$\frac{dq_n / dz}{\lambda n_{HD}\sqrt{gH_S}} = Ae^{B\frac{z}{H_S}} e^{C\frac{R_{c,1}}{H_S}} \quad (7)$$

CONCLUSIONS

For multi-level overtopping devices the phenomena of the overtopping is quite peculiar, having different behavior depending on the reservoirs´ position.

The present study demonstrated the influence that the horizontal distance *HD* has on the stored overtopping water:

- The overtopping in the lower reservoir increases while increasing *HD*.
- The overtopping in the upper reservoir decreases while increasing *HD*.
- For the specific set of tests for $HD/H_S<2$ the upper level has a big influence on the water storage on the level below. This indicates that there is a threshold after which the parameter *HD1* may increase or decrease the overall efficiency of the device.

Two different formulations (one for each reservoir) of the overtopping prediction formula by Kofoed 2002 have been derived that can take into account the *HD* parameter.
Further work will be done to analyze the reliability of the new formula and investigate the case of overtopping dependence on the parameter *HD* for 3 level overtopping device.

REFERENCES

Franco, L., de Gerloni, and L. Van der , Meer (1995): "wave overtopping on vertical and composite breakwaters". Proc. 24th International Conference of Coastal Engineering, Kobe, Japan 1, 1030-1044.

Kofoed J. P. (2002): "Wave Overtopping of Marine Structures – Utilization of Wave Energy". Ph. D. Thesis, defended January 17, 2003 at Aalborg University. Hydraulics & Coastal Engineering Laboratory, Department of Civil Engineering, Aalborg University.

Kofoed, J. P.; Frigaard, P.; Friis-Madsen, E. ; Sørensen, H. C. (2006a): "Prototype Testing of the Wave Energy Converter Wave Dragon". I: Renewable Energy. 2006 ; vol. 31, nr. 31, FEB. s. 181-189.

Kofoed, J. P. (2006b): "Vertical Distribution of Wave Overtopping for Design of Multi Level Overtopping Based Wave Energy Converters", 30th International Conference on Coastal Engineering, ICCE San Diego.

Le Méhauté, B., R. C. Y. Koh, and L. Hwang (1968) : "A systhesis of wave run-up.˝ Journal of waterways and coastal engineering division, ASCE Vol. 94 (No. WW1, proc. Paper 5807), pp. 77-92.

Mansard and Funke, 1980. E. Mansard and E. Funke, The measurement of incident and reflected spectra using a least squares method. In: Proceedings, 17th International Conference on Coastal Engineering, Sydney Vol. 1, pp. 154–172.

Frigaard, P. ; Trewers, A.; Kofoed, J. P. ; Margheritini, L. (2008):"Conceptual Design of Wave Plane". Aalborg : Aalborg University : Department of Civil Engineering, 2008. 233 s. (DCE Contract Reports; 38)

Margheritini, L. ; Vicinanza, D. ; Frigaard, P. (2008a): "SSG Wave Energy Converter : Design, Reliability and Hydraulic Performance of an Innovative Overtopping Device". I: Renewable Energy. 2009 ; vol. 34, nr. 5, 01.11.2008. s. 1371–1380

Margheritini L., Vicinanza D. And Frigaard P. (2008b): "Sea Slot Cone Generator Overtopping Performance in 3D Conditions". International Offshore and Polar Engineering Conference, ISOPE Vancouver, Canada, No 18, ISSN 1098-6189.

Van der Meer, J.W. and J. P. F. M. Janssen (1995): "wave run up and wave overtopping at dikes". Technical report, Task Committee Reports, ASCE.